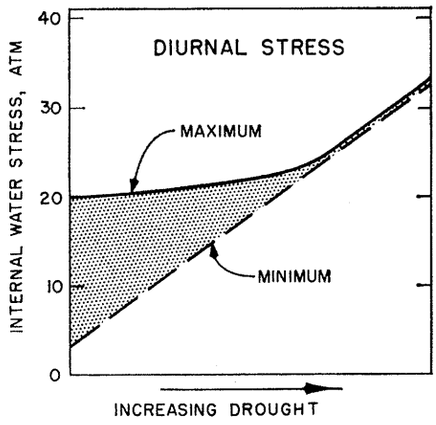

Fig. 4. Trend of internal water stress with increasing drought. Maximum values depend upon atmospheric stress and range within shaded portion of the diagram.

plateaus and for the abrupt decrease after 2:30 p.m. With water readily available, we found in other experiments that the minimum value was approached by 8:00 p.m.

By anatomical inspection, we have found that no cell divisions occur under conditions where there is no diurnal shift in water stress (Fig. 4). In Douglas fir this value is very close to 25 atm. If drought continues, the stress can increase to at least 40 atm without permanent injury to the plant. With precipitation of 3 cm or more, the diurnal pattern almost immediately returns to that in Fig. 3.

Our specific objective in constructing a pressure bomb was to evaluate a heretofore unmeasurable moisture gradient in the eastern portion of the Siskiyou Mountains of southwestern Oregon and northwestern California. Both duration and magnitude of stress are important ecologically. However, where a summer drought is common, the relation between vegetation and a moisture gradient is demonstrated by comparing the minimum internal water stess measured during the peak of the drought. The stress values for representative vegetation types shown in Table 2 are averages from three or more Douglas or Shasta fir trees (*Abies magnifica* var. *shastensis*), 1 to 2 m in height. In the same stand, other species of conifers in the same size class gave similar water stresses. Hardwoods and evergreen shrubs generally were under more stress.

Obviously, the moisture gradient is not closely related to elevation. Trees growing on very shallow soil near timberline may be under considerable stress (stand 8), while nearby trees on deeper soils are experiencing little stress (stand 1). Soils developed on serpentinite or peridotite (stand 9) are generally shallow and are characterized by higher stress values. White fir (*Abies concolor*) occurs over a wide range of elevations and temperature patterns, but was not found on sites where stress reached 25 atm. Black oak (*Quercus kelloggii*), many shrubs, and herbaceous species appear restricted to the drier sites (stands 10 and 7). The ground vegetation appears very sensitive to the entire moisture gradient, which is not surprising when one considers their more restricted root systems.

Our data represent a portion of 1500 measurements with the pressure bomb. Measurement and sampling techniques should be standardized, and more detailed comparisons with other methods of measuring water stress with different species should be made.

Table 2. Siskiyou vegetation in relation to internal water stress at peak of drought (1 September 1966). Abbreviations: BO, black oak (*Quercus kelloggii*); DF, Douglas fir (*Pseudotsuga menziesii*); ES, Englemann's spruce (*Picea engelmannii*); IC, incense cedar (*Libocedrus decurrens*); JP, Jeffrey pine (*Pinus jeffreyi*); MH, mountain hemlock (*Tsuga mertensiana*); PP, ponderosa pine (*P. ponderosa*); SF, Shasta fir (*Abies magnifica var. shastensis*); SP, sugar pine (*P. lambertiana*); WF, white fir (*A. concolor*); WP, white pine (*P. monticola*); Y, yew (*Taxus brevifolia*).

Stand No.	Elevation (m)	Vegetation*	Minimum stress (atm)
1	2040	MH-SF	3.0
2	1400	ES-DF-WF	6.5
3	1920	SF-(WP)	7.0
4	1680	WF-DF-(SP)	11.0
5	760	DF-Y-(WF)	12.5
6	1500	WF-PP-DF	14.0
7	1280	PP-DF	17.5
8	2130	MH-(SF)	19.0
9	1700	JP-IC-(DF)	19.0
10	790	DF-BO-PP	28.0

* Stand composition, listed in decreasing order of density. Species in parentheses make up less than 5 percent of total number of trees.

RICHARD H. WARING
BRIAN D. CLEARY
Forest Research Laboratory, Oregon State University, Corvallis

References and Notes

1. P. F. Scholander, H. T. Hammel, E. D. Bradstreet, E. A. Hemmingsen, *Science* **148**, 339 (1965).
2. R. O. Slatyer and W. R. Gardner, *The State and Movement of Water in Living Organisms* (Cambridge Univ. Press, London, 1965), pp. 113–129.
3. J. R. Philip, *Annu. Rev. Plant Physiol.* **17**, 245 (1966).
4. R. O. Slatyer, *ibid.* **13**, 351 (1962).
5. ———, *Australian J. Biol. Sci.* **11**, 349 (1958).

5 December 1966

Ribosomes: Effect of Interferon on Their Interaction with Rapidly Labeled Cellular and Viral RNA's

Abstract. *Rapidly labeled RNA of mouse L cells and labeled RNA of Mengo virus, unlike cellular RNA labeled under steady-state conditions, form detectable complexes with L-cell ribosomes. These ribosome-RNA complexes formed in vitro appear analogous to those assembled during polysome formation in vivo. When ribosomes are prepared from L cells exposed to homologous interferon, their capacity to associate with cell messenger is preserved, while their ability to interact with viral RNA is markedly reduced. The ribosomes from cells exposed to interferon are thus altered selectively to permit only certain messages to be bound and translated.*

When mouse L cells are infected with purified, labeled Mengo virus, the formation of the virus-specific polysome is discernible. Two events, the association of the viral RNA with a 45*S* subribosomal particle and the assembly of an approximately 250*S* polyribosomal structure, are separated in time, and the entry of viral RNA into the heavier component results in a corresponding decrease of viral RNA in the 45*S* region (*1*). These observations, with the known affinities of messenger RNA for the smaller ribosomal subunit in both animal and bacterial cells (*2, 3*), suggest that the association of viral RNA with the 45*S* particle is related to the assembly of the viral polysome. In cells exposed to homologous interferon, both the association of viral RNA with the subribosomal particle and the development of the virus-specific polysome are reduced (*1*). In a similar system (chicken embryo cells, Semliki Forest virus), interferon prevents the formation of the virus-specific polymerase (*4*) and the double-stranded RNA (*5*) formed in cells which support virus replication (*6*). Failure to assemble the viral polysome would inhibit these later steps in replication of viral RNA. Since the assembly of the virus-specific polysome is common to the replication of both DNA and RNA viruses, a blockade during assembly might explain the action of interferon against both groups of viruses. To determine whether the inhibition of the viral RNA-ribosome association in vivo represents the primary action of interferon or whether it is a reflection of some earlier alteration, we compared

the interaction of viral RNA with purified ribosomes from normal cells and from those exposed to interferon.

Interferon was prepared from mouse serum by the method of Baron and Buckler (*7*); the assays and units of activity have been described (*1, 7*). In some experiments, tissue-culture interferon at comparable levels was used. In that chicken interferon does not protect the mouse cell, it should be possible to determine the specificity of any observed effects by using both interferons.

Four liters of L cells ($\sim 4 \times 10^5$ cell/ml), strain 929, grown in suspension culture in Eagle's medium (BME) modified for spinner culture, were exposed to mouse (or chicken) interferon (10 unit/ml) for 16 hours. The cells were suspended in polysome medium [0.35*M* sucrose, 0.05*M* tris hydrochloride (*p*H 7.8), 0.025*M* KCl, 0.005*M* $MgCl_2$, and 0.006*M* mercaptoethanol] and were disrupted with a Bronson sonifier model LS-75 at a setting of 4 amperes for 12 seconds (*8*). The supernatant from the centrifugation (15,000*g*, 10 minutes) was treated with 1.2 percent sodium deoxycholate and sedimented at 105,000*g* for 4 hours through 0.5*M* sucrose (special enzyme grade, Mann Chemicals) layered over 2.0*M* sucrose (*9*). The resultant pellet was washed and resuspended in polysome medium, and the suspension was clarified by sedimentation at 10,000*g* for 10 minutes. As a further purification, some ribosome preparations were again sedimented through 2.0*M* sucrose. The final concentration of the ribosomal suspension was 3 to 6 mg/ml as measured spectrophotometrically at 258 mμ (*10*). Samples were stored at −70°C in 0.3-ml portions.

Rapidly labeled RNA was prepared by exposure of L cells to carrier-free ^{32}P phosphate (3 μc/ml) for 15 minutes. The cells were washed in cold PBS (0.01*M* PO_4 buffer *p*H 7.2, 0.85 percent NaCl) and were suspended in acetate buffer (0.01*M* acetate *p*H 5.1, 0.1*M* NaCl, and 0.0001*M* $MgCl_2$). Sodium dodecyl sulfate (0.5 percent) and bentonite (1.5 mg/ml) were added, and the suspension was mixed with aqueous phenol at 60°C for 5 minutes (*11*). The aqueous phase was again extracted with phenol, and the RNA was precipitated with two volumes of cold ethanol. The product was dissolved and precipitated three times. After the RNA was passed through Sephadex G25, the specific activity was 300 to 400 count/min per microgram. As shown by subsequent density-gradient centrifugation, the radioactivity of this product was polydisperse; it was found with fractions sedimenting from 4 to 45*S* (*3*).

Phosphorus-32-labeled Mengo RNA was prepared by exposing 2 liters of L cells to actinomycin D (1 μg/ml) for 1 hour and then to Mengo virus (multiplicity 20 : 1) at room temperature for 30 minutes. The nonadsorbed virus was removed by washing, and the cells were resuspended in phosphate-

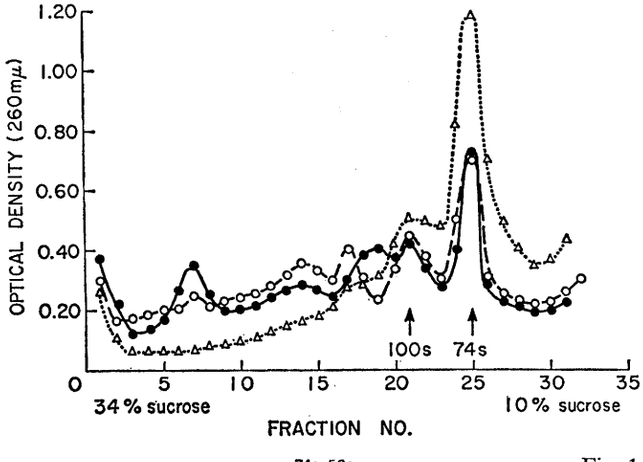

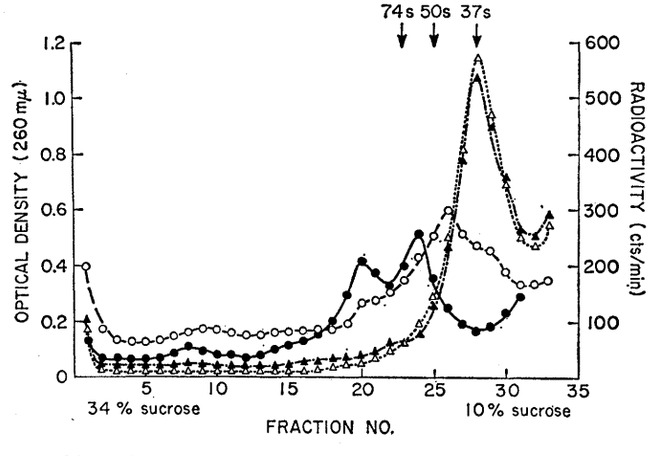

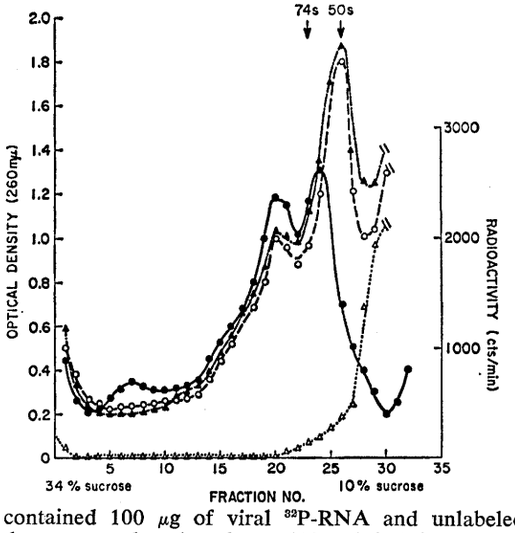

Fig. 1 (upper left). Polysome profiles from normal cells and those exposed to interferon. Polyribosomes were prepared from (i) normal cells, (ii) cells exposed to interferon (10 unit/ml, 16 hours), or (iii) cells exposed to actinomycin D (1 μg/ml, 1½ hours). Polysome pellets were gently resuspended in polysome medium and layered over linear sucrose gradients (10 to 34 percent). Samples were sedimented at 25,000 rev/min for 3 hours (SW 25.1 rotor) at −2°C. —○—○—, Optical density of normal ribosomes; —●—●—, optical density of ribosomes from cells exposed to interferon; —△—△—, optical density of normal ribosomes exposed to actinomycin D. Fig. 2 (lower left). Association of rapidly labeled RNA with ribosomes from normal cells and those exposed to interferon. Two of the reaction mixtures contained 200 μg of ^{32}P-labeled RNA and 1.2 mg of ribosomes; a third tube (control) contained 200 μg of ^{32}P-labeled RNA but no ribosomes. The mixtures were incubated for 45 minutes at 0°C and layered over linear sucrose gradients (10 to 34 percent). The tubes were sedimented for 3 hours at 25,000 rev/min. —●—●—, Optical density of normal ribosomes; —○—○—, radioactivity of cellular ^{32}P-RNA and normal ribosomes; —▲—▲—, radioactivity of cellular ^{32}P-RNA and ribosomes from cells exposed to interferon; —△—△—, radioactivity of cellular ^{32}P-RNA sedimented without ribosomes. Fig. 3 (upper right). Interaction of viral RNA with ribosomes from normal cells and those exposed to interferon. Reaction mixtures contained 100 μg of viral ^{32}P-RNA and unlabeled ribosomal RNA, and 0.6 mg of ribosomes. Ribosomes from normal cells and those exposed to interferon (10 unit/ml for 16 hours) were reacted with viral RNA at 0°C for 45 minutes. —●—●—, Optical density of normal ribosomes; —○—○—, radioactivity of normal ribosomes and viral ^{32}P-RNA; —▲—▲—, radioactivity of ribosomes from cells exposed to interferon and viral ^{32}P-RNA; —△—△—, radioactivity of viral ^{32}P-RNA sedimented without ribosomes.

free BME containing actinomycin D (2 μg/ml) and ^{32}P-phosphate (4 μc/ml). These cells were incubated at 37°C for 8 hours, and RNA was extracted from the infected cells. Approximately 0.5 mg of this product (in 2 ml) was then layered over a linear sucrose gradient (5 to 30 percent, weight/volume) containing the acetate buffer, 28 ml total volume (*12*). After centrifugation at 22,000 rev/min for 16 hours (SW 25.1 rotor), the bottom of the tube was punctured, and 0.8-ml quantities were collected. Three tubes which contained 37*S* RNA were pooled, and unlabeled ribosomal RNA of L cells was added (150 μg/ml). In the presence of 0.1*M* NaCl, the RNA was precipitated with ethanol and stored in acetate buffer at −70°C. The homogeneity of this labeled 37*S* material was similar to that of RNA obtained from the purified virus isolated by isopycnic sedimentation in CsCl (*3*).

Interactions of rapidly labeled cellular RNA and Mengo RNA with ribosomes were studied in reaction mixtures consisting of ribosomes (0.3 to 1.2 mg) and 50 to 200 μg of ^{32}P-labeled cellular RNA or ^{32}P-labeled viral RNA and ribosomal RNA in polysome medium (0.3 to 0.4 ml) adjusted to 0.005*M* NH_4Cl and 0.25*M* sucrose. Labeled RNA was the limiting component in the reaction, and ribosomes were in excess. Previous study indicated optimum association of RNA with ribosomes at 0.005*M* $MgCl_2$ (*3*). The mixtures were held at 0°C for 45 minutes with occasional gentle agitation. For analysis, the samples were layered over linear sucrose gradients (10 to 34 percent weight/volume) containing the polysome buffer and centrifuged at 25,000 rev/min for 3 hours at −2°C (SW 25.1 rotor). Fractions (approximately 0.8 ml) were collected. After the optical densities were recorded, 1 ml of water was added to each fraction, and the radioactivity was counted in Bray's solution (*13*) with a Packard liquid scintillation spectrometer. Approximately 90 to 95 percent of the radioactivity on the gradient was recovered. The monosome, used as an optical-density marker, was studied in the model E ultracentrifuge with ultraviolet and schlieren optics, and and its sedimentation coefficient s^0_{20} in 0.1*M* NaCl, 0.01*M* tris hydrochloride (*p*H 7.4), and 0.003*M* $MgCl_2$ was 74.

Exposure of L cells to homologous interferon neither alters the distribution of polysomes relative to the monomeric particles nor enriches any single polysome peak (Fig. 1). However, incubation with actinomycin D (1.0 μg/ml) for 1½ hours before harvesting ribosomes reduces the amount of heavier sedimenting polysomes and enriches the monomeric region. Ribosomes from normal cells and those exposed to interferon interact similarly with rapidly labeled cellular RNA (Fig. 2). Approximately 25 percent of the input radioactivity interacts with ribosomes, yielding a polydisperse pattern of association. Peaks of radioactivity are seen at ~ 50 and ~ 100*S*; these interactions are sensitive to cycloheximide and 2-aminoadenosine (*3*). There was no shift in optical density when RNA associated with either of the ribosome fractions; this suggests that only a small portion of the ribosomes participated in the binding of RNA. The optical density profiles were thus unaltered by exposure to interferon or reaction with RNA. Under these conditions of incubation, labeled ribosomal and transfer RNA did not associate with ribosomes (*3*).

When the abilities of these ribosome preparations to bind viral RNA were compared, large differences were detected. A large proportion (25 to 30 percent) of the input radioactivity of viral RNA entered the polysome region when ribosomes from normal cells were used, and a radioactive peak at ~ 50*S* was observed (Fig. 3) (*14*). In contrast, when ribosomes from cells exposed to interferon were used, the radioactivity entering the polysome region was only 10 to 20 percent greater than the background value for viral RNA sedimented alone (Fig. 3) and 80 to 90 percent less than the radioactivity associated with ribosomes from normal cells. Additional experiments have demonstrated that the complexes of viral RNA with ribosomes, as those of rapidly labeled cellular RNA with ribosomes, are diminished by cycloheximide (*3*). Normal ribosomes and those derived from L cells exposed to comparable amounts of the heterologous (chicken) interferon associated identically with rapidly labeled cellular and viral RNA's. Thus, the failure of ribosomes from L cells (exposed to interferon) to associate with viral RNA reflects the specific effect of the homologous protein.

When exposed to interferon, RNA and protein synthesis *de novo* is required before the antiviral state is achieved. We have found an enrichment in the newly synthesized protein of the 45*S* subribosomal particle on exposure to homologous, but not heterologous, interferon (*15*). This suggests that the actual mediator of the antiviral function, whose formation is induced by interferon, may be a ribosome-associated protein.

The enzyme fraction (*16*) obtained at *p*H 5 from cells exposed to interferon supports the translation of Mengo RNA with normal ribosomes (*17*). Combinations of these fractions and ribosome preparations from normal cells and those exposed to interferon demonstrate that the restriction in translation of Mengo RNA is only a property of the ribosomal particles. No additional inhibitors are present in the enzyme fraction. Similar observations with Sindbis virus have been made independently by Marcus and Salb (*18*). Entry ino polysomes of messenger RNA (mRNA) transcribed from vaccinia virus DNA is also blocked by interferon in vivo (*19*).

Regulation of protein biosynthesis on the polysome has now been observed in several systems from animal cells; trypsin reactivates the sluggish ribosomes found in the mitotic HeLa cell and the unfertilized egg of the sea urchin (*20*). Similar governors of polysome function may be associated with the polysomes of rat liver or the chicken embryo (*21*). The ability of the ribosome to form complexes with certain families of mRNA, while not associating with other messenger molecules, may provide a regulatory mechanism near in time and space to the product whose synthesis it controls.

WILLIAM A. CARTER
HILTON B. LEVY
National Institute of Allergy and Infectious Diseases, Bethesda, Maryland 20014

References and Notes

1. H. B. Levy and W. A. Carter, in preparation; W. A. Carter and H. B. Levy, *Fed. Proc.* **25**, 491 (1966); H. B. Levy and W. A. Carter, *Bacteriol. Proc.* 119 (1966).
2. E. Henshaw, M. Revel, H. Hiatt, *J. Mol. Biol.* **14**, 241 (1965); T. Okamoto and M. Takanami, *Biochim. Biophys. Acta* **76**, 266 (1963).
3. W. A. Carter and H. B. Levy, *Arch. Biochem. Biophys.*, in press.
4. J. Sonnabend, E. Martin, E. Mecs, K. Fantes, *J. Gen. Virol.* in press.
5. H. B. Levy, R. Friedman, W. A. Carter, in preparation.
6. R. Friedman, H. B. Levy, W. A. Carter, *Proc. Nat. Acad. Sci. U.S.* **56**, 440 (1966).
7. S. Baron and C. Buckler, *Science* **141**, 1061 (1963).
8. K. S. McCarty, J. T. Parsons, W. A. Carter, J. Laszlo, *J. Biol. Chem.* **241**, 5489 (1966).
9. F. O. Wettstein, T. Staehelin, H. Noll, *Nature* **197** 430 (1963).
10. S. T. Bayley, *J. Mol. Biol.* **18**, 330 (1966).
11. K. Scherrer and J. E. Darnell, *Biochem. Biophys. Res. Commun.* **7** 486 (1962).
12. R. J. Britten and R. B. Roberts, *Science* **131**, 32 (1960); R. Martin and B. Ames, *J. Biol. Chem.* **236**, 1372 (1961).

13. G. A. Bray, *Anal. Biochem.* **1**, 279 (1960).
14. At 0.005*M* $MgCl_2$, the ribosomal subunits are not present as discrete peaks upon density-gradient sedimentation. In the same solvent at 0.0015*M* $MgCl_2$, the subunits are found in well-defined regions (45 and 60*S*). The optical-density profiles do not suggest that many 45*S* subunits are available for binding; apparently, there is a strong preference for binding to this particle even over intact ribosomes.
15. H. B. Levy and W. A. Carter, in preparation.
16. E. B. Keller and P. C. Zamecnik, *J. Biol. Chem.* **221**, 45 (1956).
17. W. A. Carter and H. B. Levy, in preparation.
18. P. I. Marcus and J. M. Salb, *Virology* **30**, 502 (1966).
→ W. K. Joklik and T. C. Merigan, *Proc. Nat. Acad. Sci. U.S.* **56**, 558 (1966).
→ J. Salb and P. I. Marcus, *ibid.* **54**, 1353 (1965 → A. Monroy, R. Maggio, A. M. Rinaldi, *ibid.*, p. 107.
21. M. B. Hoagland, O. A. Scornik, L. C. Pfefferkorn, *ibid.* **51**, 1184 (1964); R. Soeiro and H. Amos, *Science* **154**, 662 (1966).

30 December 1966

Tetraethylammonium Ions: Effect of Presynaptic Injection on Synaptic Transmission

Abstract. *Tetraethylammonium ions were injected into the presynaptic axon of the squid giant synapse. Injection of these ions caused prolongation of the action potential with decreased outward current. The prolonged spike was associated with increased release and prolonged activity of the transmitter substance. Although the amplitude of the postsynaptic potential increased with presynaptic depolarization, strong depolarization blocked transmitter release. In the injected presynaptic axon, transmitter release was blocked by 10^{-6} gram of tetrodotoxin per milliliter. Transmitter release appears to be under control of presynaptic potential levels.*

The relation of an action potential arriving at a presynaptic terminal to the ensuing release of transmitter has not been fully elucidated. Depolarization of the presynaptic terminal where inward current has been blocked by addition of tetrodotoxin is a sufficient stimulus for transmitter release (*1*).

The action of tetraethylammonium ions (TEA) on electrogenesis of axonal action potentials has been thoroughly studied (*2*). Intracellular injection of TEA produces prolonged spikes with diminution and even elimination of the outward K^+ current (K^+ activation) normally present following initial rapid depolarization of the action potential. Furthermore, TEA causes an increase of transmitter release at synapses (*3*). We have examined the effects of TEA-induced presynaptic potential changes on this release.

The giant synapse of the squid provides an excellent preparation for the study of the mechanism coupling the action potential with transmitter release (*4, 5*). The electrical properties of the postsynaptic axon have been thoroughly studied, but the presynaptic fiber is itself large enough to be impaled with several microelectrodes.

The stellate ganglion, together with the pre- and postsynaptic nerves, of the common squid (*Loligo paelii*) available at Woods Hole was freed by dissection. The preparation was cleaned and placed in a chamber through which oxygenated, cooled (20°C) sea water was run. Two microelectrodes filled with 1*M* potassium citrate were placed postsynaptically less than 0.5 mm from the synapse. One microelectrode containing potassium citrate and another filled with 1*M* tetraethylammonium chloride were placed in the presynaptic axon as close as possible to its terminal. The isolated preparation could be studied for periods up to 10 hours.

Before ejection of TEA from its microelectrode, normal synaptic function was studied. A directly evoked presynaptic action potential produced by outward current through a microelectrode led to a depolarizing, excitatory postsynaptic potential (PSP) and usually to triggering of the postsynaptic spike. Further depolarization of the presynaptic axon produced incremental increases in the maximum voltage of the presynaptic spike with accompanying increases in the PSP amplitude. Intense rectification following the presynaptic spike normally prohibited prolonged steady-state depolarization beyond 30 mv. No change in the time course of the PSP accompanied such prolonged low-level presynaptic depolarization. Orthodromically invaded presynaptic spikes were, on the other hand, attenuated by depolarization, resulting in depression of the PSP amplitude (*5*).

Extracellularly applied TEA did not produce clearcut effects; however, after TEA was injected into the presynaptic axon by iontophoresis with currents up to 10^{-6} amp for periods as long as 5 hours, prolongation of the presynaptic action potential was observed (Fig. 1). Such prolongations (TEA spike) increased with increasing duration of applied TEA. Stronger currents appeared to damage the presynaptic fiber. Accompanying the spike prolongation, there was either no change in the properties of the membrane at rest or, at most, a slight decrease in

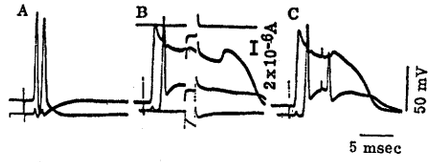

Fig. 1. Development of TEA spikes. (A) Control presynaptic (upper trace) and postsynaptic (lower trace) response to orthodromic stimulation. (B) Responses after iontophoretic injection of TEA into presynaptic axon, showing prolongation of the presynaptic spike; the postsynaptic spike is followed by a prolonged PSP associated with a conductance increase of the postsynaptic fiber tested by a current pulse. Top trace shows current monitor, and bottom trace shows response of the resting membrane of the postsynaptic fiber to applied current. (C) An antidromically invaded postsynaptic spike during a prolonged PSP is greatly attenuated by the increased conductance of the postsynaptic membrane.

conductance. During the plateau of the prolonged action potential, membrane conductance was almost indistinguishable from that found in the resting condition. Current-voltage studies showed that the usual rectification in the depolarizing direction was greatly reduced or eliminated by intracellular application of TEA. These changes are similar to those produced in experiments where TEA is introduced by pressure (*2*). No changes in the electrical properties of the postsynaptic axon were produced by presynaptic administration of TEA. To prevent initiation of postsynaptic action potentials and nonlinearities in PSP amplitude produced by conductance changes related to depolarization we studied small PSP's, or we used background postsynaptic hyperpolarization. Therefore, the PSP can be considered a measure of transmitter release.

The TEA spike was accompanied by an increase in PSP size and a prolongation of the PSP. The PSP persisted throughout the duration of the presynaptic spike and terminated milliseconds after the termination of the TEA spike. The prolonged PSP was associated with an increased conductance and related changes in spike electrogenesis shown both by application of pulses of current (Fig. 1B) and by incomplete invasion and shunting of an antidromic spike (Fig. 1C).

In the presence of TEA, large depolarizations of the presynaptic fiber were possible. Increasing presynaptic depolarization produced a graded increase in the PSP amplitude until a maximum was reached with depolariza-